Thickness-Dependent Thermal Transition Temperatures in Thin Conjugated Polymer Films†

M. Campoy-Quiles,‡ M. Sims,‡ P. G. Etchegoin,§ and D. D. C. Bradley*,‡

Ultrafast Photonics Collaboration, Carbon Based Electronics Consortium and Experimental Solid State Physics Group, Blackett Laboratory, Imperial College London, South Kensington, London SW7 2BZ, U.K., and The MacDiarmid Institute for Advanced Materials and Nanotechnology, and School of Chemical and Physical Sciences, Victoria University of Wellington, PO Box 600, Wellington, New Zealand

Received March 14, 2006; Revised Manuscript Received July 17, 2006

ABSTRACT: We report the effects that geometrical confinement has on both the glass transition temperature, T_g, and the crystalline phase transition temperature, T_c, for two widely studied conjugated polymers, namely poly(9,9-dioctylfluorene) [PFO] and poly(9,9-dioctylfluorene-*co*-benzothiadiazole) [F8BT]. The T_g and T_c values were determined for thin film samples via temperature-dependent ellipsometry measurements. The thickness-dependent T_g (T_c) behavior is characterized by three regimes, namely, (i) large d or bulk samples for which $T_g = T_g^{bulk}$ ($T_c = T_c^{bulk}$), (ii) intermediate d samples for which $T_g > T_g^{bulk}$ (likewise for T_c), and (iii) ultrathin samples for which T_g drops again (likewise for T_c). The intermediate regimes occur for 160 nm > d > 60 nm and 300 nm > d > 80 nm for PFO and F8BT, respectively. The higher-than-bulk T_g and T_c values offer the potential to design more robust and thermally stable polymer optoelectronic devices, including light-emitting diodes, lasers, and solar cells.

Introduction

The condensed phase behavior of polymer glasses is dependent upon the ability of the constituent molecules to undergo large-scale cooperative motions (α-relaxation). The glass transition temperature, T_g, marks, in simplest terms, the temperature at which the elastic modulus (and viscosity) of the polymer glass falls and hence at which α-relaxation becomes more probable. A polymer's ability to become rubberlike can, however, be affected by local variations in the interaction with its surroundings, e.g., near to a substrate interface. The wetting properties of a particular substrate can then play a central role in determining a local T_g. In situations where interfacial forces are attractive they can act to inhibit cooperative dynamics and lead to a rise in T_g. On the other hand, the extra mobility afforded to polymer chains by a relaxation of constraints at a "free" surface may reduce T_g, especially, for instance, if there is a segregation of chain ends to the surface and a consequent reduction in packing density. Deviations from bulk thermodynamic properties should not then be surprising when the polymer film thickness acts to confine motions on characteristic molecular length scales. For example, the dependence of T_g on film thickness has been extensively investigated[1−4] in nonconjugated polymer films such as poly(methyl methacrylate) (PMMA) and polystyrene (PS) (for a review see ref 5). Low molecular weight glass formers[6−8] have been similarly studied. In most cases, there is an apparent depression in polymer T_g with decreasing film thickness.[1−5,9] Confinement effects typically onset at d < 40−60 nm in PS, although this value is reported to depend on parameters such as polymer molecular weight[4] and chain stiffness.[10] Such behavior has been related to an enhanced free volume (lower T_g) afforded by a relaxation in chain mobility constraints at the polymer−air interface[3] coupled with relatively weak polymer−substrate interactions. This is especially clear in studies of free-standing PS films, which show a much more pronounced reduction in T_g than for films supported on SiO_x substrates.[2] Interestingly, the T_g depression in PS shows little dependence on the type of substrate used.[5] On the other hand, the thickness dependence of T_g in other polymers has been shown to be very sensitive to the type of substrate used. For example, T_g in poly(2-vinylpyridine) (P(2)PV) increases with decreasing film thickness when films are spin-coated onto the oxide surface of a Si wafer.[11] It has also been shown that the T_g of isotactic-PMMA films can either increase or decrease as a function of decreasing film thickness depending on whether the polymer is deposited on an aluminum or a silicon surface.[12]

Very recently, nonmonotonic variations with thickness (where both $T_g > T_g^{bulk}$ and $T_g < T_g^{bulk}$ are found for the same polymer over different thickness ranges) have been reported for thin films of PS and PS derivatives when probed with shear-modulated scanning force microscopy.[13] Ellison et al.[10] have correspondingly encouraged the study of polymer systems with physicochemical properties distinct from typical PS and PMMA test bed samples in order that a better understanding of the range of behaviors and the underlying physical processes can be developed. These authors have also focused attention on the need to consider nonuniformity in T_g across the thickness of a film: Any suppression or enhancement in T_g is not expected to be a uniform effect since the interactions that control it are clearly nonuniform.[10,13,14]

Many of the studies to date have been motivated by the importance to advances in technology of an understanding of the behavior of polymers on ever decreasing length scales. The as yet largely unpredictable behavior of confined polymer systems has implications for a wide range of applications. In addition to the already mentioned variations in T_g, there are documented variations in melting point,[14] chain diffusion,[9] intrinsic viscosity,[9] electrical insulation,[15] optical anisotropy,[16] and film morphology and moisture uptake.[17] Here, we are particularly interested in understanding confinement effects

† Based in part on a presentation to the American Physical Society March Meeting, 2005.

‡ Imperial College London.

§ Victoria University of Wellington.

* Author for correspondence: e-mail D.Bradley@imperial.ac.uk.

10.1021/ma0605752 CCC: $33.50
Published on Web 10/03/2006

within the context of thin-film-based ($d \sim 100$ nm), substrate-supported, conjugated polymer optoelectronic devices, a seemingly unstudied territory in this framework (but see refs 16 and 18). A lowering of T_g comparable to that seen in many nonconjugated polymer films of similar thickness would likely be highly detrimental to device stability, a key parameter for commercial adoption of the technology.

Since the first report of electroluminescence emission from a poly(*p*-phenylenevinylene) light-emitting diode,[19] the conjugated class of polymers has attracted increasing attention as a material system well-suited to use in displays and lighting, thin film transistor based electronic circuits, solar cells and photodetectors, and lasers and amplifiers. The polyfluorene family, in particular, has been the subject of intense research interest due to its excellent charge transport properties and the tunability of its emission (both spontaneous and stimulated) across the entire visible spectrum.[20−22] While the bulk thermal properties of a number of conjugated polymers are documented (see for example refs 23 and 24 for PFO and F8BT, respectively), the effects of confinement thereon remain (as far as we are aware) unreported. Here we present an ellipsometry study of thickness-dependent confinement effects on the glass transition temperature, T_g, and on the crystallization temperature, T_c, of poly(9,9-dioctylfluorene) [PFO] and poly(9,9-dioctylfluorene-*co*-benzothiadiazole) [F8BT] thin film samples spin-coated on fused silica substrates. Ellipsometry is a technique that is well suited to the study of thin film properties, including dielectric function and thickness,[25] morphology,[26] and T_g:[1,2] It has the required sensitivity and can be implemented in a scanning modality with ~50 μm lateral resolution. We have recently shown[27,28] that ellipsometry can also be employed to measure crystalline phase transition temperatures and that by selection of an appropriate probe wavelength (within the transparency window of the polymer under study) a depth-averaged measurement of T_g and/or T_c can be obtained. We find here that the thickness-dependent T_g (T_c) behavior for PFO and F8BT is characterized by three regimes, namely, (i) large d or bulk samples for which $T_g = T_g^{bulk}$ ($T_c = T_c^{bulk}$), (ii) intermediate d samples for which $T_g > T_g^{bulk}$ (likewise for T_c), and (iii) ultrathin samples for which T_g drops again (likewise for T_c). The intermediate regimes occur for 160 nm > d > 60 nm and 300 nm > d > 80 nm for PFO and F8BT, respectively. We discuss the thickness-dependent T_g results in terms of three literature models: These consider (a) an excess free volume at the air/polymer interface,[1] (b) an attractive interaction with the substrate and a reduced T_g at the surface,[3] and (c) interfacial interactions that are mediated on a characteristic length scale.[17] The attainment of higher-than-bulk T_g and T_c values that we report offers the potential to design more robust and thermally stable polymer optoelectronic devices.

Experimental Section

Poly(9,9-dioctylfluorene) [PFO] and poly(9,9-dioctylfluorene-*co*-benzothiadiazole) [F8BT], with a typical degree of polymerization $n \approx 100$, were obtained from The Dow Chemical Co. (see Scheme 1). These polymers had been subjected to rigorous purification procedures at Dow to remove residual catalyst and other impurities and were used as supplied. Thin films were spin-coated onto clean fused silica substrates from solutions of PFO and F8BT dissolved in toluene. Spectrosil B fused silica substrates (Kaypul Optics Limited) were subjected to ultrasonic cleaning in acetone (~15 min) and 2-propanol (~15 min) and finally dried using nitrogen gas. This cleaning procedure, which is commonly used when fabricating organic-based devices, is expected to lead to slightly hydrophobic surfaces. Different concentrations (in the range 0.77−40 g/L) and different spin speeds (in the range 2000−4000 rpm but only for F8BT) were used to allow a wide range of polymer film thicknesses (10 nm < d < 320 nm for PFO and 40 nm < d < 3590 nm for F8BT) to be prepared: A constant spin-coating time of 40 s was used in all cases. Ellipsometric scans were performed with a SOPRA GES-5 rotating polarizer, reflection mode ellipsometer with its incidence angle set at 60° to the surface normal (close to the Brewster angle of the substrate) and an incident wavelength (550 nm for PFO and 600 nm for F8BT) selected to lie within the polymer's long wavelength transparency region.[29] Each sample was held in vacuo at ~10^{-7} mbar within a turbomolecular-pumped chamber in order to avoid any oxidation during heating, an environment that also promotes the removal of any residual solvent from the film. The temperature was ramped from 25 to 150 °C at a rate of 0.7 °C/min using a Lakeshore temperature controller. The ellipsometric angles (tan Ψ and cos Δ) were recorded at 10 s intervals during the heating cycle. Linear fits were performed for each set of data (each sample) over three temperature ranges: (i) 25 °C < T < ($T_g - \Delta T$), (ii) $T_g + \Delta T < T < T_c - \Delta T$, and (iii) $T > T_c + \Delta T$. T_g and T_c were determined from the intersection points for the linear fits to ranges (i) and (ii) and (ii) and (iii), respectively. ΔT was varied from 5 to 20 °C in order to estimate the error in T_g and T_c. These errors (δT_g and δT_c) were usually between 1 and 3 °C, while typical standard deviations for the linear fits were around 1.5×10^{-4}. We note that the sample-to-sample variation in T_g and T_c is <2 °C or, in other words, that the deduced phase transition temperatures are sample-to-sample reproducible within the observed experimental error limits.

Scheme 1. Chemical Structures of (a) Poly(9,9-dioctylfluorene) [PFO] and (b) Poly(9,9-dioctylfluorene-*co*-benzothiadiazole) [F8BT]

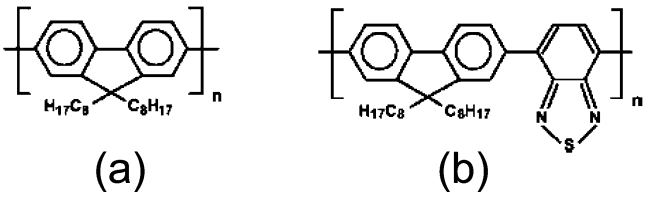

Control experiments were performed at room temperature in air in which the ellipsometric angles of a PFO film were monitored over an extended period (more than 10 h). The wavelength was fixed (550 nm), and the incidence angle was scanned from 61° to 69°. TanΨ and cos Δ did not change, within the experimental error (typically <0.003), throughout this extended measurement interval (see Figure 1). This indicates that the small but finite UV component of the ellipsometer's Xe lamp output does not degrade our polymer films in any significant way. It further demonstrates that the α relaxation time at room temperature for these materials is much longer than the typical measurement time (~3 h). This can be easily appreciated by comparing Figure 1 with Figures 2, 3, and 4.

To try and ensure the removal of any solvent trapped within deposited polymer films, some researchers studying confinement

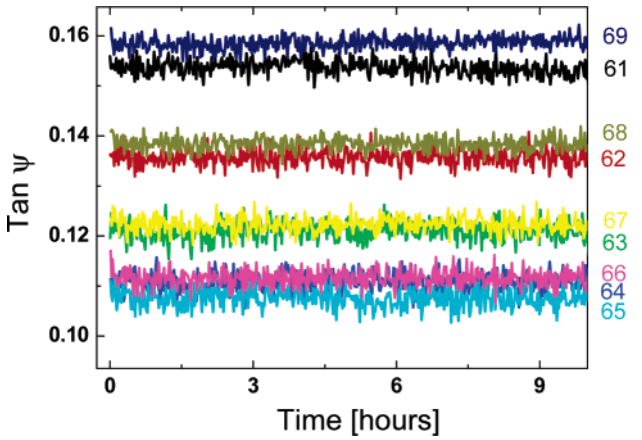

Figure 1. Extended time dependence of tan Ψ measured for a ~100 nm PFO film for nine different incidence angles.

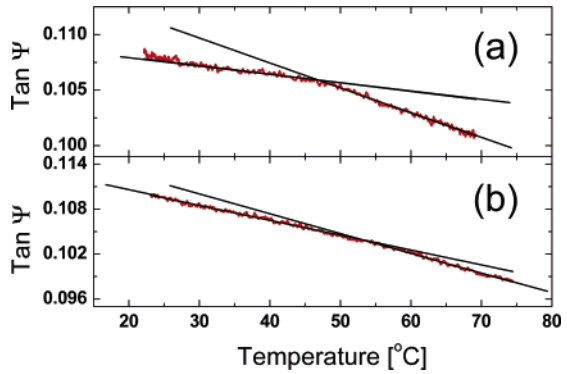

Figure 2. Tan Ψ as a function of temperature for a ~60 nm thick PFO film (a) as spin-coated and (b) after slow cooling from 68 °C. Straight lines are linear fits to the experimental data before and after T_g.

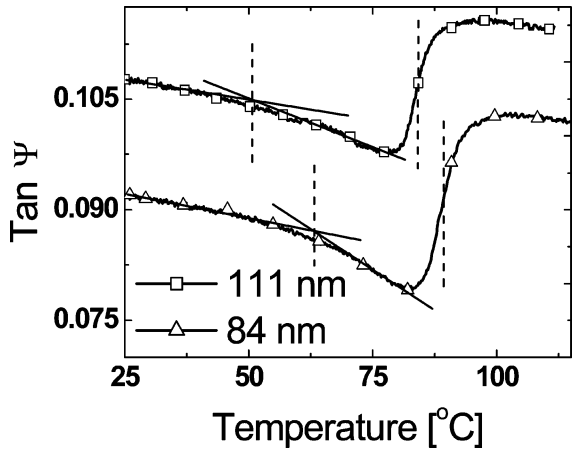

Figure 3. Typical temperature-dependent ellipsometric scans for 84 nm (open triangles) and 111 nm (open squares) thickness PFO films. The first change in the tan Ψ slope (~50 °C, identified for each film thickness by a dashed vertical line drawn through the crossing point of the corresponding straight line asymptotes) can be assigned to the glass transition temperature, T_g. The sudden increase in tan Ψ (~90 °C) indicates crystallization, and we take T_c to be the point of steepest slope (also identified by a dashed vertical line). It is evident that both T_g and T_c differ for the two film thicknesses.

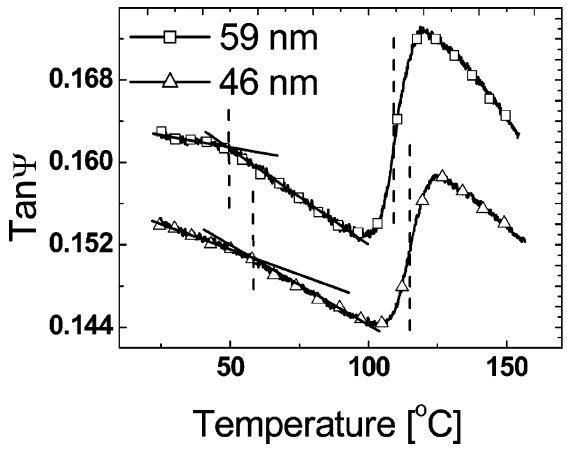

Figure 4. Typical temperature-dependent ellipsometric scans for 46 nm (open triangles) and 59 nm (open squares) thickness F8BT films. Similar features to those seen in Figure 1 allow identification of T_g (~55 °C) and T_c (~115 °C) and again show that the transition temperatures differ for the two film thicknesses.

effects in supported polymer systems perform an annealing step prior to embarking on a measurement of T_g. This typically consists of heating the samples above the glass transition temperature and then quenching back to room temperature before the detailed measurements are undertaken. Significant polymer relaxation has been reported for spin-coated PMMA films upon such annealing, resulting in an important film thickness reduction.[30,31] In our study premeasurement annealing treatments of this type have not been applied to the polymer films, since:

(a) The default treatment for optoelectronic devices with conjugated polymer active layers is that they are not annealed, and therefore, by not preannealing our films, the results retain their greatest relevance to the corresponding device-oriented research community. We note however that more specific studies might well ensue in which the effects of a particular fabrication protocol (choice of polymer molecular weight, solvent, solution concentration, deposition method (spin-coating, ink-jet printing, etc.), substrate and surface preparation, etc.) on T_g and/or T_c are carefully examined, but this goes beyond the scope of the present initial investigation.

(b) While PS, PMMA, and related materials form amorphous glassy films, the polyfluorenes considered in this study are semicrystalline. Hence, taking the spin-coated films above T_g leads to crystallite formation and irreversibly changes the film morphology and thermodynamic response. Taking this to its extreme, annealing will eventually eliminate T_g. Moreover, as the morphology changes the polymer films will become further and further removed from those found within pristine optoelectronic device structures, and hence any results will become of less and less practical relevance to strategies for device stability optimization.

To check whether solvent-mediated relaxation plays a significant role, we have carried out several control experiments. A PFO film with an ellipsometrically deduced initial thickness of 85 ± 1 nm was heated to 68 °C (above T_g) at a rate of 0.7 °C/min and slowly cooled at <0.7 °C/min: The thickness of the film after heating and cooling was 83 ± 1 nm. The relative departure from the equilibrium volume, $\gamma = (d_{\text{spin-coated}} - d_{\text{annealed}})/d_{\text{annealed}}$, is in this case 0.02 ± 0.02, namely, 5−6 times smaller than reported for PMMA films of the same thickness.[30] In terms of the changes in T_g, Figure 2 shows the temperature dependence of tanΨ for two ~60 nm thick PFO films on heating from room temperature: (a) presents the data for an as-spin-coated film (film A), and (b) presents the data for a film that after spin-coating had been first heated to and then slowly cooled from 68 °C (above T_g) back to room temperature (film B). There is a slight increase in the value of T_g deduced for film B (52 ± 3 °C) relative to film A (48 ± 2 °C), but the two values lie within each other's error bars. In addition, the change in tanΨ slope at T_g is reduced for film B relative to that for film A. Both effects (the small increase in T_g and the smoothing of the tan Ψ kink) can be attributed to crystallite formation, without needing to invoke solvent loss. Measurements of the temperature evolution of tan Ψ for (what we expect to be) solvent-free, glassy PFO films quenched from the isotropic melt (~220 °C) show a less well resolved change in slope at T_g but still have a strong feature at T_c. We find that, just as for the results presented below for as-spin-coated samples, the T_c of PFO films quenched from the melt shows a nonmonotonic dependence on film thickness. The weakened evidence for T_g in the ellipsometry scans on our melt-quenched films may simply be an indication of the difficulty in completely avoiding crystallization during the quenching process. Another drawback with respect to melt-quenched samples is that they are not typically used within optoelectronic devices since their preparation is not obviously compatible with device fabrication requirements: The melt temperatures are typically rather high (300 °C ≥ T ≥ 150 °C). This means that studies on such samples would not provide information of relevance to optimizing polymer device stability, which is one of the major motivations for our study.

Our control experiments on melt-quenched samples, together with the small variations in T_g and thickness, d, upon annealing as-spin-coated films at 68 °C, indicate that solvent trapping and subsequent elimination would not be expected to play a significant role in the thickness dependence of the phase transition temperatures described in this study. We note, in addition, that the amount of trapped solvent in thin films should increase with increasing film thickness,[30] and, therefore, a mechanism based on trapped solvent would only be able to explain a monotonic dependence of T_g on film thickness

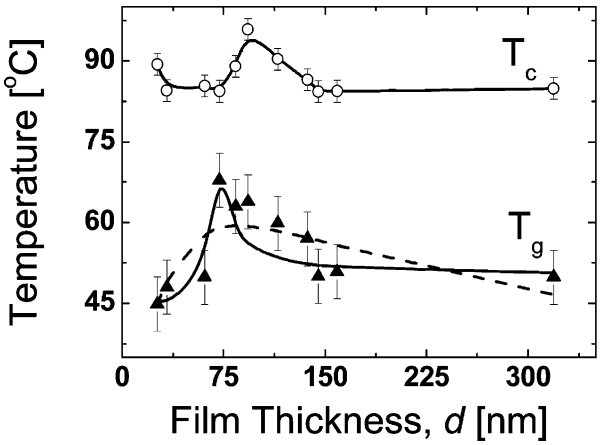

Figure 5. Ellipsometrically deduced T_g (solid triangles) and T_c (open circles) values plotted as a function of PFO film thickness. For thicknesses between 60 and 159 nm, both T_g and T_c are greater than their bulk values. PFO films with thicknesses smaller than 60 nm show T_g smaller than T_g^{bulk} and an increase in T_c for $d < 20$ nm. The dashed and solid lines correspond to fits of the experimental data using eqs 2 and 3, respectively.

with T_g decreasing as the thickness increased. We note also that the close correspondence in nonmonotonic behavior for T_g and T_c would not be expected if trapped solvent were important since the slow heating (0.7 °C/min) in vacuo (10^{-7} mbar) would be expected to significantly affect the amount, if not fully remove, any trapped solvent (toluene) over the temperature interval ($\Delta T > 30$ °C) between T_g and T_c.

Additional spectroscopic (250−850 nm, 5 nm steps) ellipsometry measurements were taken before and after each heating cycle. This was done in order to evaluate the film thickness before and after heating as well as to check the changes in the absorption spectrum related to crystallization. The spectroscopic data were analyzed using the standard critical point model, in which the dielectric function is described as a sum of excitons (3 for PFO and 4 for F8BT).[29] Each exciton (i) is characterized by a set of four parameters: central energy (E_{ci}), width (Γ_i), amplitude (A_i), and excitonic phase (ϕ_i), as previously reported.[26,29,32]

Results and Discussion

Figure 3 shows typical ellipsometric angle (tan Ψ)[25] vs temperature scans for 111 nm (open squares) and 84 nm (open triangles) thickness PFO films: These are representative of a large number of scans for a wide range of different film thicknesses (cf. Figure 5). A comparison with differential scanning calorimetry (DSC) measurements ($T_g^{DSC} \sim 50$ °C, heating at 20 °C/min after quenching from 220 °C)[23] allows us to assign the first change in slope (δ tan $\Psi/\delta T$) at ∼50−63 °C to the glass transition temperature, just as often done to identify T_g for saturated polymer films.[1−4] We have recently demonstrated that the temperature dependence of tan Ψ is closely linked to the film density (ρ),[27,28,32] such that changes in the slope of tan Ψ at T_g are equivalent to changes in $\delta\rho/\delta T$ (or the expansion coefficient) between the glassy and rubbery states. A similar comparison with DSC measurements ($T_c^{DSC} \sim 93$ °C)[23] identifies the abrupt increase in tan Ψ at ∼90 °C with the onset of crystallization:[27] We assign the tan Ψ(T) inflection point temperature as T_c (in analogy to a peak heat flow in DSC). The step change in tan Ψ is also accompanied by a rapid densification of the film and an increase in the integrated photoluminescence (PL) intensity emitted normal to the film plane, effects that are readily attributed to the crystallization process.[27] The crystalline phase has its own characteristic PL spectral features so that both intensity and spectral measurements as a function of temperature can be used as complementary methods to determine T_c.[27,33] It is evident from Figure 3 that both T_g and T_c increase ($\Delta T \sim 12$ °C and $\Delta T \sim 5$ °C, respectively) upon reduction of the PFO film thickness from 111 to 84 nm ($\Delta d \sim 30$ nm).

Ellipsometry scans were also used to determine the thin film T_g and T_c values for F8BT, for which polymer the bulk thermal properties have been previously characterized by DSC measurements ($T_c^{DSC} \approx 130$ °C for samples heated following quenching from the melt).[24] Figure 4 shows two representative tan Ψ vs temperature scans for films of thickness 59 nm (open squares) and 46 nm (open triangles). The tan Ψ vs temperature variation for F8BT is seen to follow a similar behavior to that for PFO with a slope change in tan Ψ around T_g (∼50−65 °C) and an abrupt increase in the value of tan Ψ around T_c (∼115 °C). Here, T_g (T_c) increases by an amount $\Delta T \sim 4.5$ °C (∼5 °C) upon reduction of the F8BT thickness from 59 to 46 nm ($\Delta d \sim$ 13 nm).

Figure 5 shows ellipsometrically determined T_g (solid triangles) and T_c values (open circles) for 11 different PFO film thicknesses in the range 10 nm $< d <$ 320 nm. We note that it is easier to determine T_c (hence the smaller error bars) because the change in tan Ψ is more abrupt at T_c than at T_g. As the film thickness is reduced from 320 nm (increasing confinement) T_g (T_c) starts to increase at $d \sim 159$ nm and rises to a local maximum, T_g^{max} (T_c^{max}), at $d \sim 70$ nm (∼90 nm), some 18 °C (11 °C) higher than the corresponding bulk or thick film value. On further reducing d, the T_g value decreases and reaches a value ∼5 °C lower than T_g^{bulk} for films with $d \sim 18$ nm. These results identify two film thickness ranges in which T_g has values that are distinct from the bulk: (i) an intermediate region (60 nm $< d <$ 160 nm) for which $T_g > T_g^{bulk}$ and (ii) an ultrathin region ($d <$ 60 nm) for which $T_g < T_g^{bulk}$. In contrast to T_g the crystalline transition temperature drops from its maximum value at $d \sim 90$ nm to a value $\approx T_c^{bulk}$ for $d \sim$ 25−75 nm but then rises above the bulk value on going to even thinner ($d <$ 20 nm) films. The good agreement between the bulk values of the glass transition temperature deduced using DSC[23] (after quenching from 220 °C) and ellipsometry, both equal to 50 ± 3 °C, suggests that the amount of solvent trapped within our polymer films (after they have been placed in vacuo within a turbomolecularly pumped sample chamber for measurement) is relatively small compared to other materials such as PMMA.[30] We further note that PL intensity measurements reveal a similar nonmonotonic dependence of T_g and T_c upon PFO film thickness, consistent with the ellipsometry studies reported here. The details of this parallel PL-based investigation will be described elsewhere.

It is notable that the variation in T_g is almost twice as large as that for T_c, which suggests that nanoconfinement has a more pronounced effect on the properties that govern the glass transition. Our current ellipsometry set up did not allow us to reach the temperature, T_m, at which the films melt into the nematic liquid crystalline mesophase ($T_m \sim 180$ °C), but T_m could be clearly measured via photoluminescence measurements.[27] Interestingly, the PL deduced T_m values showed very little variation (within the experimental error of 2−3 °C) for film thicknesses across the full range studied here (10−320 nm).

Figure 6 shows the corresponding ellipsometrically determined T_g (triangles) and T_c (circles) data for 10 F8BT films over an extended thickness range from 40 to 3590 nm. For greater clarity in the region of interest, a logarithmic abscissa (thickness) scale has been employed. Note that thick (>500 nm) films are more readily prepared with good optical quality for

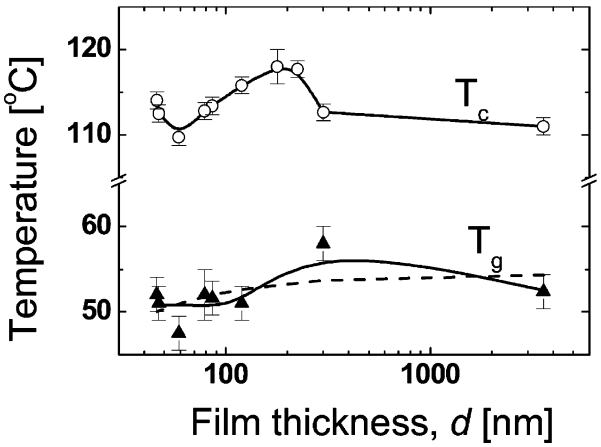

Figure 6. Ellipsometrically deduced T_g (solid triangles) and T_c (open circles) values plotted as a function of F8BT film thickness. For thicknesses between 80 and 300 nm, both T_g and T_c are greater than their bulk values. F8BT films with thicknesses around 60 nm show T_g smaller than T_g^{bulk}. Higher-than-bulk T_g and T_c values were found for $d < 40$ nm. The dashed and solid lines correspond again to fits of the experimental data using eqs 2 and 3, respectively.

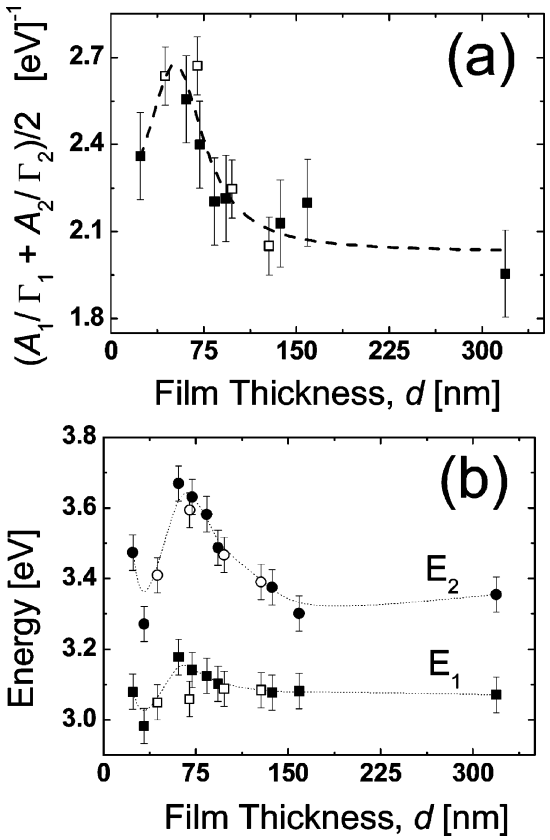

Figure 7. Thickness dependence of standard critical point model parameters of the dielectric function for as-spin-coated PFO films: (a) the summed exciton amplitude-to-width ratios for the two excitons needed to fit the ellipsometry data in the long wavelength absorption peak range and (b) the central energies E_1 and E_2 for these two excitons. Open symbols represent additional data obtained for samples spin-coated from *p*-xylene solutions and are included for comparison. The lines are provided as a guide to the eye.

F8BT than for PFO. In the latter case, thick films are typically somewhat opaque due to scattering effects. The glass and crystalline transition temperatures of F8BT films also exhibit a nonmonotonic dependence on *d*, but the deviations from bulk behavior are less pronounced than for PFO, even though they begin at greater thickness ($d \sim 300$ nm compared to 159 nm for PFO). Reductions in thickness lead initially to an increase

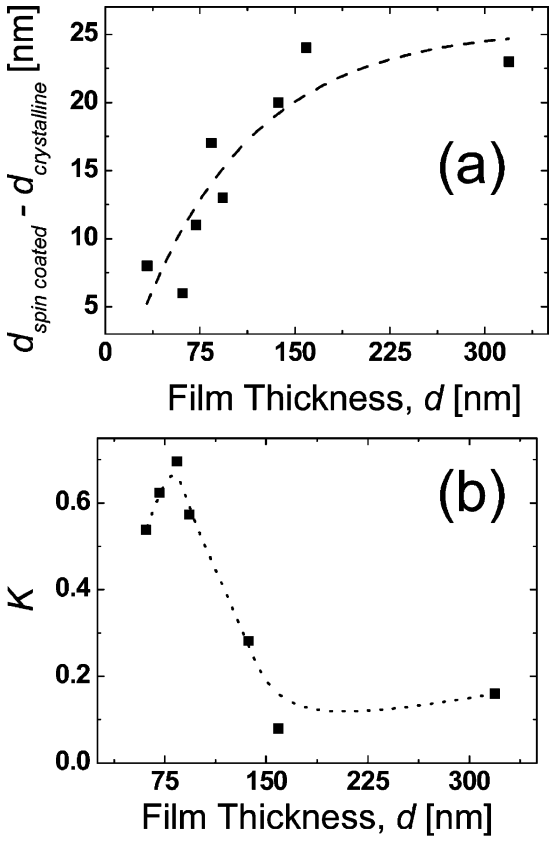

Figure 8. (a) Dependence of the crystallization-induced decrease in PFO film thickness on the initial, as-spin-coated, film thickness. (b) Thickness dependence of *K* (cf. eq 1) for PFO films. In both cases the lines are provided as a guide to the eye.

in both T_g and T_c, as per PFO, but here T_g^{max} (T_c^{max}) is only some 5 °C (8 °C) above T_g^{bulk} (T_c^{bulk}). T_g and T_c then decrease with decreasing thickness until below $d \sim 60$ nm, $T_g < T_g^{bulk}$ and $T_c < T_c^{bulk}$. Even thinner films ($d < 40$ nm) exhibit $T_g \geq T_g^{bulk}$ and $T_c > T_c^{bulk}$. The thickness range over which $T_c > T_c^{bulk}$ spans from 80 to 300 nm in our F8BT films, while it is only 72 to 140 nm in the corresponding PFO films.

One observation concerning the data in Figures 5 and 6 is that the thickness onset for a deviation from bulk behavior for PFO ($d \sim 159$ nm) and F8BT ($d \sim 300$ nm) is considerably larger than that typically reported for PS ($d \sim 40-60$ nm). Interestingly, Ellison et al.[10] have recently demonstrated that modification of the polymer repeat unit from styrene to 4-*tert*-butylstyrene can result in a shift in the thickness onset for deviations from bulk behavior to $d \sim 350$ nm. These authors proposed that the increased chain stiffness in poly(4-*tert*-butylstyrene) plays a key role in the observed shift, a proposal that is qualitatively consistent with our findings: The conjugated PFO and F8BT chains are certainly more stiff than PS chains.

An analysis of the spectroscopic ellipsometry data for the as-spin-coated conjugated polymer films demonstrates that their electronic properties may also be significantly altered by thin film confinement. The ellipsometry data allow a determination of the in-plane dielectric function[26] at room temperature as a function of film thickness. This in turn allows an estimate of the corresponding variation in density: Integration of the imaginary part of the dielectric function gives the oscillator strength that, in the absence of any changes in the transition dipole moment orientation distribution, is expected to be proportional to the material density. When using excitonic peaks,[29] the oscillator strength is proportional to the sum of the ratios between amplitude and width for each peak, i.e., $\sum_i A_i/\Gamma_i$.

Figure 7a shows this sum for the two exciton peaks in the visible region of PFO. The oscillator strength again shows a nonmonotonic dependence with film thickness, with a maximum at $d \sim 70$ nm. This might suggest that $T_g > T_g^{bulk}$ for intermediate thicknesses arises from a higher average density in this range (but note the dipole moment orientation complication in respect of the connection between oscillator strength and density). The excitonic energies also exhibit a nonmonotonic dependence on d, with blue-shifted peaks in the same intermediate thickness range. The blue shift would usually be taken to indicate a reduction in average conjugation length, but a more detailed study is needed to better understand the origin of the observed exciton oscillator strength and peak energy changes.

The crystallization of the PFO films is accompanied by a densification:[27] The decrease in room temperature film thickness upon annealing ranges from $\Delta d \sim 25$ nm to $\Delta d \sim 5$ nm, when going from thick ($d \sim 319$ nm) to thin ($\sim$40 nm) films, respectively (see Figure 8a). In terms of the dielectric function parameters, the exciton amplitudes increase, their peak widths broaden, and their central positions red shift, in agreement with previously published results.[33] An increase in oscillator strength is also seen for all of the samples upon crystallization. While these trends are common to all PFO film thicknesses, a greater effect is observed for thinner films than for bulk samples. It is possible to quantify the overall changes in absorption using the normalized difference in the spectrally integrated values of the ellipsometrically deduced extinction coefficients, defined as

$$K = \frac{\int_{250\,nm}^{450\,nm} |K_{crystalline} - K_{spin-coated}| d\lambda}{\int_{250nm}^{450nm} |K_{spin-coated}| d\lambda} \qquad (1)$$

Figure 8b shows the dependence of K on film thickness and again there is a nonmonotonic variation, here with K_{max} at $d \sim 90$ nm. These results further confirm that the electronic properties of conjugated polymer thin films are also significantly affected by confinement, mirroring the film thickness variation seen for T_g and T_c.

The spectral changes with thickness and upon crystallization are similar in the case of F8BT films. The only major difference compared to PFO films is that the F8BT films do not appear to shrink upon crystallization: Ellipsometrically deduced film thicknesses for the as spin-coated and crystalline films lie within each other's experimental errors. This might be the result of a higher density for F8BT films with respect to PFO films, as also suggested by the deduced higher refractive index in the transparency region.[29]

We next discuss our results in terms of existing models for the effects of nanoconfinement on the phase transition temperatures of supported polymer thin films. The nonmonotonic variation of T_g or T_c with thickness d has not been widely reported for other polymers. However, Ellison and Torkelson did find such behavior for PS films supported on silica when selectively probing T_g of the uppermost $\sim$14 nm via a PL-labeling technique.[34] In addition, Sills and co-workers also found a nonmonotonic dependence of T_g with d for PS and a cross-linkable styrene−vinylbenzocyclobutene copolymer.[13] They used a shear-modulated scanning force microscopy technique to determine T_g, a method that probes a near surface region of order 1 nm thickness. The nonmonotonic variation was proposed to arise as a consequence of the combined effect of structuring at the substrate interface and interdiffusion between this interfacially modified layer and the unperturbed bulk structure.[13] Three structural regions would then be expected: (i) an interfacial region in which spin-coating related shear forces induce chain extension and/or disentanglement, (ii) an intermediate region wherein the polymer chains are highly entangled, and (iii) an unperturbed bulk region. A similar conceptual picture might also explain our findings, despite the fact that nonresonant ellipsometry (i.e., in the transparent region) averages over the whole film thickness. Two interesting points from Sills et al.'s study are that increasing molecular weight apparently shifts the T_g peak toward larger thicknesses and that the onset thickness for deviations from bulk behavior is significantly higher in this report ($d \sim 250$ nm) than determined from other measurements ($d \sim 40-60$ nm[2,4]). In the interest of completeness, it is worth pointing out that while some authors have reported a molecular weight dependence of the T_g variation with thickness for supported PS films,[2,4,13] other groups have found molecular weight independent results.[5,10] The discrepancy might simply be due to the use of different annealing treatments[10] and/or different measurement protocols, e.g., T_g measured on cooling[2,4] rather than on heating.[5,10]

An alternative model to that of Sills et al.[13] had been previously proposed by Kim et al.:[3] their continuous multilayer model (CMM) is based on dividing the polymer film into an infinite number of sublayers, each with a different glass transition temperature. The CMM air−polymer surface was characterized by a lower T_g than the bulk, while close to the substrate, a higher T_g was assumed due to polymer/substrate attractive interactions. The CMM then provides an explicit expression for the average $T_g(d)$ expected (by means of the mean value theorem) for a film of thickness d:

$$T_g(d) = T_g^{bulk}\left(\frac{d(2k+d)}{(\xi+d)^2}\right) \qquad (2)$$

where k and ξ are two adjustable length-scale parameters that respectively account for the substrate−polymer and air−polymer interactions. We note that although this model was developed to explain the (at that time) exclusively monotonic T_g vs d variation reported in the literature, it does allow for a nonmonotonic T_g vs d profile, provided that $k > 2\xi$. The latter inequality requires that the effect of the polymer−substrate interface should (in this model) propagate at least twice as deep into the film as the effect of the air−polymer interface. The CMM thus contrasts with a number of other empirical models that only describe a monotonic decrease in T_g with decreasing d, the result of higher chain mobility at the air/polymer interface. For example, the empirical relation of Keddie, Jones, and Cory,[1] namely $T_g(d) = T_{g,bulk}[1 - (\alpha/d)^\delta]$ (with fitting parameters α and δ), does not allow a local minimum/maximum. It is clear that substrate interactions need to be included in order to be able to describe sufficiently well the effects of geometric confinement on T_g.

Our data can be fit using eq 2 (the dashed line in Figures 5 and 6), but the deduced bulk T_g value (e.g., $T_g^{bulk} = 25$ °C for PFO) and the thickness at which $T_g = T_g^{bulk}$ (e.g., $d \sim 250$ nm for PFO) are in fact quite unreasonable. This reveals an additional limitation, namely that the polymer/air and polymer/substrate interface interactions are assumed to act in a particular direction: They are assumed to decrease and increase T_g, respectively. The CMM would clearly need to be modified to cover the case where the substrate interaction is strong but repulsive. We note that neutron scattering experiments for polyfluorenes deposited on ITO-coated substrates have been interpreted in exactly that way with low-density sublayers of around 2 nm proposed to exist at the polymer/substrate

interface.[35] These considerations highlight the complexity of behavior that can arise and hence the flexibility needed for a suitably general model.

A substantially better fit to our experimental data can be obtained using the $T_g(d)$ relationship derived by Zhou et al.:[36]

$$T_g(d) = \frac{T_g^{bulk}}{2}\left[\exp\left(-\frac{\alpha_1 - 1}{d/d_0 - 1}\right) + \exp\left(-\frac{\alpha_2 - 1}{d/d_0 - 1}\right)\right] \quad (3)$$

where α_1 and α_2 are dimensionless adjustable parameters that account for polymer/substrate and polymer/air interface effects, respectively, and d_0 represents a characteristic phase transition length (which might be related for instance to the degree of polymerization/molecular weight, the average chain end-to-end distance, or the length scale for cooperative motion).[17,36] Compared to eq 2, eq 3 is mathematically symmetric with respect to the effects of the interfaces (i.e., $T_g(d)$ depends equally on α_1 and α_2). Note also that eq 3 allows the character of the interaction at both interfaces to be either attractive (leading to a higher-than-bulk $T_g(d)$) or repulsive (leading to a lower-than-bulk $T_g(d)$) depending on the particular values of α_1 and α_2: For $d > d_0$, $\alpha_i > 1$ (<1) leads to T_g reducing (enhancing) interactions. Fits of our experimental data to eq 3 (cf. solid lines in Figures 5 and 6) resulted in smaller standard deviations than found for fits to eq 2 (χ^2 is reduced 1.4 and 2.9 times for PFO and F8BT, respectively). The good (moderate) agreement between eq 3 (eq 2) and the experimental trends (compared to monotonic $T_g(d)$ profiles) demonstrates that substrate/polymer interactions are relatively more important in polyfluorene-on-spectrosil substrates than for PS spin-coated on Si. In addition, the introduction of a characteristic system length scale over which properties change (eq 3) helps to improve the fit.

The fact that the variation with d of the crystalline phase transition temperature, $T_c(d)$, does not map exactly on to that for T_g is consistent with the two transitions being governed to differing degrees by variations in a number of polymer parameters, including chain conformation and dynamics.[37] In particular, the increase in T_c for the thinnest films can simply be due to a shortage of material to form crystallites. It is worth noting that tan $\Psi(T)$ scans for films with $d \leq 10$ nm did not show the characteristic step change at T_c seen in Figures 3 and 4 for thicker films. Likewise, no step change in photoluminescence intensity was seen in PL(T) scans for films with thicknesses $d < 10$ nm. This may be consistent with a suppression of crystallization as for poly(*p*-xylylene)[17] and poly(di-*n*-hexylsilane),[38] but it might simply signify a sensitivity limit for the two techniques.[5] The strong PL signal observed for ultrathin polyfluorene films does not seem to support the latter hypothesis. A better understanding of the processes that lead to nonmonotonic T_g and T_c vs d profiles for polyfluorene thin films on substrates is currently being sought. The relative roles of the polymer/substrate interaction and the air/polymer interface are clearly important to understand. A systematic study of the effect of molecular weight might also provide useful insights.

Finally, one should note that the $T_g(d)$ and $T_c(d)$ behavior presented here offers a potentially useful tool for the optimization of conjugated polymer based optoelectronic device stability: It is clearly desirable that the polymer components of such devices retain as constant a morphology as possible over time in order to ensure reliable performance. It might be argued that glassy phases have the advantage of morphological homogeneity leading for instance to spatially uniform charge injection/transport and recombination. They may not be ideal, however, from the perspective of long-lived device performance under external or internal heating. Spin-coated films typically possess a nonequilibrium structure that is frozen-in during solvent loss as the T_g of the residual solvent/polymer mixture rises above ambient temperature. Morphological instabilities are then expected and not just in situations where the film temperature rises above T_g: Polymers also undergo physical aging below T_g via conformational/structural relaxation (β-relaxation) processes. The ability to select an active layer thickness in an LED or laser,[39−42] or for that matter in any other device, for which T_g can be elevated relative to the bulk value is then an attractive proposition. It will also be interesting to study physical aging below T_g in more detail for conjugated polymer films: Recent studies show significant changes in aging properties for ultrathin PS and PMMA films[43,44] with, under certain circumstances, a dramatic suppression of aging. It would be highly desirable to be able to achieve the same result for conjugated polymer thin films within device structures. Semicrystalline morphologies also offer an opportunity for enhanced thermal stability,[28,45] but the accompanying increase in heterogeneity (nonmonodomain samples) and rigidity (embrittlement) can cause problems. In general terms the bulk T_g values of polymer semiconductors should be kept high to ensure stability but a more complete understanding of the influence of spatial confinement and interface interactions within device structures could prove equally valuable. Conversely, a reduction in T_g near an interface (leading to enhanced cooperative motion and more free volume) should be avoided since it is likely to be detrimental to long-term device stability for a number of reasons, including (1) reduced adhesion, (2) enhanced percolation of external ions and/or interdiffusion of polymer chains, and (3) greater susceptibility to damage during vacuum deposition of metal electrodes.

Conclusions

We have investigated the influence of film thickness on the thermal transition temperatures of conjugated polymer layers spin-coated on spectrosil substrates. Comparison was made between the experimentally determined $T_g(d)$ and $T_c(d)$ variations and the predictions of literature models.[3,36] We found nonmonotonic changes in both T_g and T_c with decreasing film thickness. Deviations from bulk behavior were first observed for PFO when $d < 159$ nm and for F8BT when $d < 300$ nm. As the film thickness was further reduced, we observed a thickness range in which $T_g > T_g^{bulk}$ and $T_c > T_c^{bulk}$, namely 60 nm $\leq d \leq$ 159 nm for PFO and 80 nm $\leq d \leq$ 300 nm for F8BT, with $\Delta T \leq 20$ °C. For even thinner PFO films ($d < 60$ nm), we found T_g to decrease below T_g^{bulk}, but T_c increased above T_c^{bulk} again. In the case of F8BT, both T_g and T_c increase for $d < 40$ nm. A more detailed analysis of spectroscopic ellipsometry data suggests that there may be a higher-than-bulk density for films that lie within the intermediate thickness region characterized by enhanced T_g and T_c values. These findings motivate a careful reconsideration of device design strategies for enhanced thermal stability, a process that will necessitate extensive measurements of T_g and T_c within specific state-of-the-art device structures for which a variety of electrode interface constructions, and surface treatments as well as active layer thicknesses should be explored. The potential rewards in terms of enhanced device lifetime should however be sufficient to encourage such a detailed study to be undertaken.

Acknowledgment. We thank the UK Engineering and Physical Sciences Research Council for financial support through the Ultrafast Photonics Collaboration programme (GR/R55078) and the CBE Initiative (GR/R97085). We also thank The Dow Chemical Co. for providing the polyfluorene polymers

CDV

that we have studied, and we thank the Sumation Chemical Co., Ltd., for permission to publish this work: Sumation now holds the rights to the Lumation family of polyfluorenes and should be contacted for any future enquiries thereon.

References and Notes

(1) Keddie, J. L.; Jones, R. A. L.; Cory, R. A. *Europhys. Lett.* **1994**, *27*, 59.
(2) Forrest, J. A.; Dalnoki-Veress, K.; Dutcher, J. R. *Phys. Rev. E* **1997**, *56*, 5705.
(3) Kim, J. H. Jang, J.; Zin, W. *Langmuir* **2000**, *16*, 4064.
(4) Singh, L. Ludovice, P. J.; Henderson, C. L. *Thin Solid Films* **2004**, *449*, 231.
(5) Roth, C. B.; Dutcher, J. R. *J. Electroanal. Chem.* **2005**, *584*, 13.
(6) Jackson, C. L.; McKenna, G. B. *J. Non-Cryst. Solids* **1991**, *131*, 221.
(7) Arndt, M.; Stannarius, R.; Groothues, H.; Hempel, E.; Kremer, F. *Phys. Rev. Lett.* **1997**, *79*, 2077.
(8) Wang, L. M.; He, F.; Richert, R. *Phys. Rev. Lett.* **2004**, *92*, 095701.
(9) Forrest, J. A. *Eur. Phys. J. E* **2002**, *8*, 261.
(10) Ellison, C. J.; Mundra, M. K.; Torkelson, J. M. *Macromolecules* **2005**, *38*, 1767.
(11) Van Zanten, J. H.; Wallace, W. E.; Wu, W. *Phys. Rev. E* **1996**, *53*, R2053.
(12) Sharp, J. S.; Forrest, J. A. *Phys. Rev. E* **2003**, *67*, 031805.
(13) Sills, S.; Overney, R. M.; Chau, W.; Lee, V. Y.; Miller, R. D.; Frommer, J. *J. Chem. Phys.* **2004**, *120*, 5334.
(14) Kim, J. H.; Jang, J. S.; D-Lee, Y.; Zin, W. *Macromol. Rapid Commun.* **2001**, *22*, 386.
(15) Liang, T.; Makita, Y.; Kimura, S. *Polymer* **2001**, *42*, 4867.
(16) Zhokhavets, U.; Gobsch, G.; Hoppe, H.; Sariciftci, N. S. *Thin Solid Films* **2004**, *451*, 69.
(17) Huang, H. L.; Xu, Y. G.; Low, H. Y. *Polymer* **2005**, *46*, 5949.
(18) Gray, T.; Buenviaje, C.; Overney, R. M.; Jenekhe, S. A.; Zheng, L. X.; Jen, A. K. Y. *Appl. Phys. Lett.* **2003**, *83*, 2563.
(19) Burroughes, J. H.; Bradley, D. D. C.; Brown, A. R.; Marks, R. N.; Mackay, K.; Friend, R. H.; Burns, P. L.; Holmes, A. B. *Nature (London)* **1990**, *347*, 539.
(20) Redecker, M.; Bradley, D. D. C.; Inbasekaran, M.; Woo, E. P. *Appl. Phys. Lett.* **1999**, *74*, 1400.
(21) Campbell, A. J.; Bradley, D. D. C.; Antoniadis, H. *Appl. Phys. Lett.* **2001**, *79*, 2133.
(22) Heliotis, G.; Bradley, D. D. C.; Turnbull, G. A.; Samuel, I. D. W. *Appl. Phys. Lett.* **2002**, *81*, 415.
(23) Grell, M.; Bradley, D. D. C.; Inbasekaran, M.; Woo, E. P. *Adv. Mater.* **1997**, *9*, 798.
(24) Grell, M.; Redecker, M.; Whitehead, K. S.; Bradley, D. D. C.; Inbasekaran, M.; Woo, E. P.; Wu, W. *Liq. Cryst.* **1999**, *26*, 1403.
(25) Azzam, R. M. A.; Bashara, N. M. *Ellipsometry and Polarized Light*; Elsevier North-Holland, Inc.: Amsterdam, 1977.
(26) Campoy-Quiles, M.; Etchegoin, P. G.; Bradley, D. D. C. *Phys. Rev. B* **2005**, *72*, 045209.
(27) Sims, M.; Zheng, K.; Campoy-Quiles, M.; Xia, R.; Stavrinou, P. N.; Etchegoin, P. G.; Bradley, D. D. C. *J. Phys.: Condens. Matter* **2005**, *17*, 6307.
(28) Campoy-Quiles, M. Sims, M.; Zheng, K.; Etchegoin, P. G.; Bradley, D. D. C., submitted for publication.
(29) Campoy-Quiles, M.; Heliotis, G.; Xia, R.; Ariu, M.; Pintani, M.; Etchegoin, P. G.; Bradley, D. D. C. *Adv. Funct. Mater.* **2005**, *15*, 925.
(30) Richardson, H.; López-García, Í.; Sferrazza, M.; Keddie, J. L. *Phys. Rev. E* **2004**, *70*, 051805.
(31) de Gennes, P. G. *Eur. Phys. J. E* **2002**, *7*, 31.
(32) Campoy-Quiles, M.; Etchegoin, P. G.; Bradley, D. D. C. *Synth. Met.* **2005**, *155*, 279.
(33) Ariu, M.; Lidzey, D. G.; Bradley, D. D. C. *Synth. Met.* **2000**, *111*, 607.
(34) Ellison, C. J.; Torkelson, J. M. *Nat. Mater.* **2003**, *2*, 695.
(35) Mitchell, W. J.; Burn, P. L.; Thomas, R. K.; Fragneto, G.; Markham, J. P. J.; Samuel, I. D. W. *J. Appl. Phys.* **2004**, *95*, 2391.
(36) Zhou, H.; Kim, H. K.; Shi, F. G.; Zhao, B.; Yota, J. *Microelectron. J.* **2002**, *33*, 221.
(37) Durell, M.; Macdonald, J. E.; Trolley, D.; Wehrum, A.; Jukes, P. C.; Jones, R. A. L.; Walker, C. J.; Brown, S. *Europhys. Lett.* **2002**, *58*, 844.
(38) Frank, C. W.; Rao, V.; Despotopoulou, M. M.; Pease, R. F. W.; Hinsberg, W. D.; Miller, R. D.; Rabolt, J. F. *Science* **1996**, *273*, 912.
(39) Grice, A. W.; Bradley, D. D. C.; Bernius, M. T.; Inbasekaran, M.; Wu, W. W.; Woo, E. P. *Appl. Phys. Lett.* **1998**, *73*, 629.
(40) Whitehead, K. S.; Grell, M.; Bradley, D. D. C.; Jandke, M.; Strohriegl, P. *Appl. Phys. Lett.* **2000**, *76*, 2946.
(41) Heliotis, G.; Xia, R. D.; Turnbull, G. A.; Andrew, P.; Barnes, W. L.; Samuel, I. D. W.; Bradley, D. D. C. *Adv. Funct. Mater.* **2004**, *14*, 91.
(42) Xia, R.; Heliotis, G.; Stavrinou, P. N.; Bradley, D. D. C. *Appl. Phys. Lett.* **2005**, *87*, 031104.
(43) Kawana, S. Jones, R. A. L. *Eur. Phys. J. E* **2003**, *10*, 223.
(44) Priestley, R. D.; Broadbelt, L. J.; Torkelson, J. M. *Macromol.* **2005**, *38*, 654.
(45) MacDonald, W. A. *J. Mater. Chem.* **2004**, *14*, 4.

MA0605752